

## Superhydrophobic metallic glass surface with superior mechanical stability and corrosion resistance

J. Ma, X. Y. Zhang, D. P. Wang, D. Q. Zhao, D. W. Ding, K. Liu, and W. H. Wang

Citation: [Applied Physics Letters](#) **104**, 173701 (2014); doi: 10.1063/1.4874275

View online: <http://dx.doi.org/10.1063/1.4874275>

View Table of Contents: <http://scitation.aip.org/content/aip/journal/apl/104/17?ver=pdfcov>

Published by the [AIP Publishing](#)

---

### Articles you may be interested in

[Patterned superhydrophobic surface based on Pd-based metallic glass](#)

Appl. Phys. Lett. **101**, 081601 (2012); 10.1063/1.4747327

[Facile creation of bio-inspired superhydrophobic Ce-based metallic glass surfaces](#)

Appl. Phys. Lett. **99**, 261905 (2011); 10.1063/1.3672036

[Wetting of bulk metallic glass forming liquids on metals and ceramics](#)

J. Appl. Phys. **110**, 043508 (2011); 10.1063/1.3615630

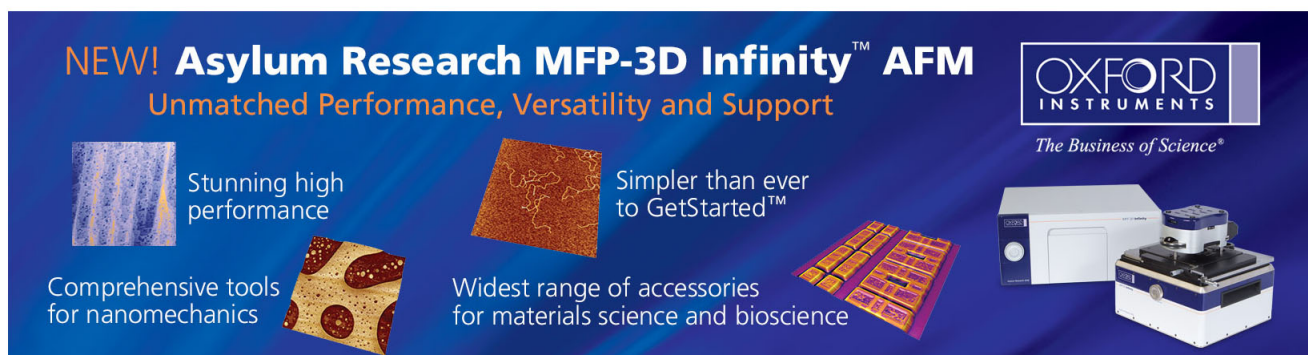
[Calculating glass-forming ability in absence of key kinetic and thermodynamic parameters](#)

Appl. Phys. Lett. **97**, 024102 (2010); 10.1063/1.3462315

[Correlation between corrosion performance and surface wettability in ZrTiCuNiBe bulk metallic glasses](#)

Appl. Phys. Lett. **96**, 251909 (2010); 10.1063/1.3429591

---

This is a promotional banner for the Asylum Research MFP-3D Infinity AFM. The background is a dark blue gradient. On the left, the text 'NEW! Asylum Research MFP-3D Infinity™ AFM' is written in white and orange, followed by the tagline 'Unmatched Performance, Versatility and Support' in orange. Below this, there are four distinct sections: 1) 'Stunning high performance' with a blue-tinted AFM image; 2) 'Simpler than ever to GetStarted™' with a brown-tinted AFM image; 3) 'Comprehensive tools for nanomechanics' with a yellow-tinted AFM image; and 4) 'Widest range of accessories for materials science and bioscience' with a yellow-tinted AFM image. On the right side, the Oxford Instruments logo is displayed in white, with the slogan 'The Business of Science®' underneath. At the bottom right, a photograph of the MFP-3D Infinity AFM instrument is shown.

## Superhydrophobic metallic glass surface with superior mechanical stability and corrosion resistance

J. Ma,<sup>1</sup> X. Y. Zhang,<sup>2</sup> D. P. Wang,<sup>1</sup> D. Q. Zhao,<sup>1</sup> D. W. Ding,<sup>1</sup> K. Liu,<sup>2,a)</sup> and W. H. Wang<sup>1,a)</sup>

<sup>1</sup>*Institute of Physics, Chinese Academy of Sciences, Beijing 100190, People's Republic of China*

<sup>2</sup>*Key Laboratory of Bio-Inspired Smart Interfacial Science and Technology of Ministry of Education, School of Chemistry and Environment, Beihang University, Beijing 100191, People's Republic of China*

(Received 25 December 2013; accepted 21 April 2014; published online 29 April 2014)

Superhydrophobic surface with mechanical stability and corrosion resistance is long expected due to its practical applications. We show that a micro-nano scale hierarchical structured Pd-based metallic glass surface with superhydrophobic effect can be prepared by the thermoplastic forming, which is a unique and facile synthesis strategy for metallic glasses. The superhydrophobic metallic glass surface without modification of low surface energy chemical layer also exhibits superior mechanical stability and corrosion resistance compared with conventional superhydrophobic materials. Our results indicate that the metallic glass is a promising candidate superhydrophobic material for applications. © 2014 AIP Publishing LLC. [<http://dx.doi.org/10.1063/1.4874275>]

Recently, superhydrophobic surfaces have been extensively studied due to their importance in fundamental research and practical applications.<sup>1–6</sup> In nature, many biological materials exhibit excellent surface superhydrophobicity, such as lotus leaves, rice leaves, butterfly wings, mosquito compound eyes, etc.<sup>2,7,8</sup> However, few related products were launched using such surfaces due to their susceptibility to mechanical contact and corrosion during normal uses, such as finger contact, abrasive wear, and acid-base chemical solutions.<sup>5,6,9–12</sup> And the limited mechanical durability and corrosion resistance have been identified as the main barriers to practical application of superhydrophobic materials, because the mechanical wear or corrosion applied on the superhydrophobic surfaces could destroy the surface roughness features that are essential for superhydrophobicity.<sup>5,10,13,14</sup> Actually, quite a large proportion of existing superhydrophobic surfaces are obtained by being modified with a low surface energy layer (e.g., fluoroalkylsilane) on them,<sup>15,16</sup> and the mechanical contact or chemical corrosion could be a disaster to the contributing modified layer or even the substrate, and cause a decline in their non-wetting property. Although a great number of superhydrophobic metallic surfaces have been successfully fabricated,<sup>17–19</sup> these artificial superhydrophobic metallic surface structures usually can be easily destroyed, resulting in the disappearance of the superhydrophobicity due to their poor mechanical properties, which is severe obstacle for the practical applications of superhydrophobic metallic surfaces.<sup>20</sup> Therefore, seeking a proper material with superior properties to mitigate the mechanical and corrosion damage is urgent and crucial for the practical use of superhydrophobic surface.

Metallic glasses (MGs) are a class of metallic materials without long-range ordering structures, which endows them with unique properties such as ultrahigh strength and hardness, high wear and corrosion resistances, etc.<sup>17–21</sup> More amazingly, MGs can be thermoplastically formed like plastics because their viscosity drops dramatically with the

increase of temperature in their supercooled liquid region (SLR), which is a temperature window between glass transition temperature  $T_g$  and crystallization temperature  $T_x$ .<sup>22–26</sup> A number of processing methods have been developed to process MGs for the preparation of complex surface structures with well-defined geometry and shape on length scales ranging from nano, micro, to macro.<sup>22,23,27–29</sup> Benefiting from such advantages, MGs are regarded as the desirable materials for miniature-fabrication and such precise, convenient, and low-cost approach could significantly extend their practical applications.<sup>22,23,29–35</sup> However, some MGs such as Ce-based MG are readily oxidizable material, which are very unstable in environment and needed surface modification by low surface energy layer;<sup>15,23</sup> some MGs have poor mechanical stability and corrosion resistance, and their superhydrophobic surfaces<sup>36,37</sup> cannot be applied in practical. In the present work, we report the design and fabrication of multi-scale structures for inducing a superhydrophobic behavior on the intrinsically hydrophilic Pd-based MG surface through the thermoplastic forming approach. These superhydrophobic MG surfaces exhibited superior mechanical stability and corrosion resistance, which could extend the practical applications of MG materials.

The PdNiCuP bulk glassy alloy has good flow properties and be thermal stable in its SLR, which meet the requirements for thermoplastic forming.<sup>36</sup> The PdNiCuP MG rod with a diameter of 5 mm was prepared from a master alloy with nominal composition of Pd 40 at. %, Ni 10 at. %, Cu 30 at. %, and P 20 at. % by conventional water cooled copper mould casting. The rod was cut into a thickness of 1 mm and then the surface was polished by the abrasive paper and polishing machine for the thermoplastic forming. It needs two steps to fabricate the micro-nano hierarchical structures on the surface of MGs, as illustrated in Fig. 1. Step one [Figure 1(a)] is the nano-scale surface structure fabrication, and the MG plate was first stacked with an anodic aluminum oxide (AAO) template that has a nano-scale structures on the surface and heated into its SLR ( $=620\text{ K}$ ),<sup>28</sup> then a 60 MPa force was provided. After removing the AAO template, we got Pd-based MG surface with nano-scale structure. Step two

<sup>a)</sup>Authors to whom correspondence should be addressed. Electronic addresses: whw@aphy.iphy.ac.cn and liuks@buaa.edu.cn

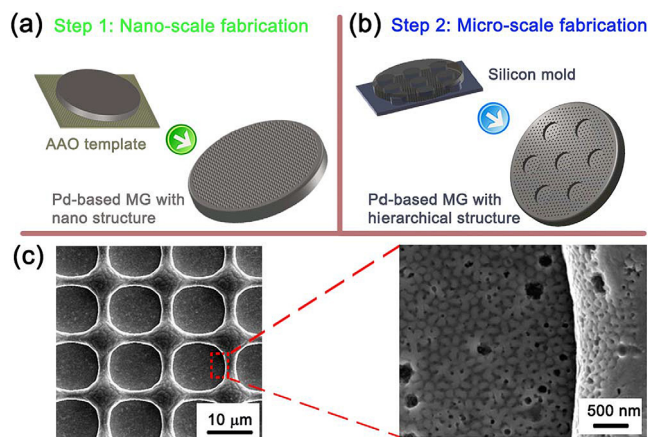


FIG. 1. Schematic diagram of the fabrication of micro-nano scale structured superhydrophobic metallic glass surface. (a) Step one: nano scale fabrication with AAO template; (b) step two: micro scale fabrication with silicon mold; (c) SEM images of the as-fabricated MG surface (left) and the magnified details (right).

[Figure 1(b)] is the micro-scale fabrication process, the same process in step one was repeated, but the used silicon mold has micro-scale patterns and the applied force was 10 MPa. Thus, the Pd-based MG surface with micro-nano hierarchical structures was obtained. The scanning electron microscopy (SEM) images of the as-fabricated MG surface are presented in Fig. 1(c). We can see the uniformly distributed periodic pore patterns [the left image in Fig. 1(c)] on the surface of the MG, and the diameter and periodicity of these pores are about  $12\ \mu\text{m}$  and  $14\ \mu\text{m}$ , respectively. The highlighted dashed rectangular in left image in Fig. 1(c) shows that the nano-scale structures with a mean diameter of  $\sim 80\text{--}100\ \text{nm}$  decorating on the micro pore patterns [in the right image of Fig. 1(c)]. This two step fabrication method can effectively and controllably prepare the hierarchical structure patterns over two orders of magnitude on the MG surface.

The water contact angles (CAs) were measured by a contact angle system (DataPhysics OCA20) and a charge-coupled device camera system at room temperature. Figure 2(a) shows an image of a water drop ( $2\ \mu\text{l}$  in volume) on the original polished MG wafer, and the CA is about  $52^\circ$ , indicating the intrinsic hydrophilicity of the original Pd-based MG surface. However, the case significantly changes when the MG surface was decorated with the micro-nano hierarchical structure. The CA increases sharply to  $156^\circ$  [Figure 2(b)], and the water droplet deposited on the surface forms almost perfect sphere. The drastic change of CAs indicates that the formed micro-nano scale hierarchical structures by thermoplastic forming play a critical role in the resultant superhydrophobicity. Interestingly, the superhydrophobic surface also shows high adhesive force to the liquid drop. It can be seen from Figs. 2(c) and 2(d) that the water drop adheres to the MG surface firmly even it is tilted for  $90^\circ$  and  $180^\circ$ . Figure 2(e) gives the comparison photos of water drops (about  $50\ \mu\text{l}$  in volume) on the polished and structured surfaces of MG. We can see that the water droplet collapses on the polished surface, while the structured one exhibits the superhydrophobic effect.

The wettability of a solid surface is usually governed by its surface free energy and surface geometrical structures.

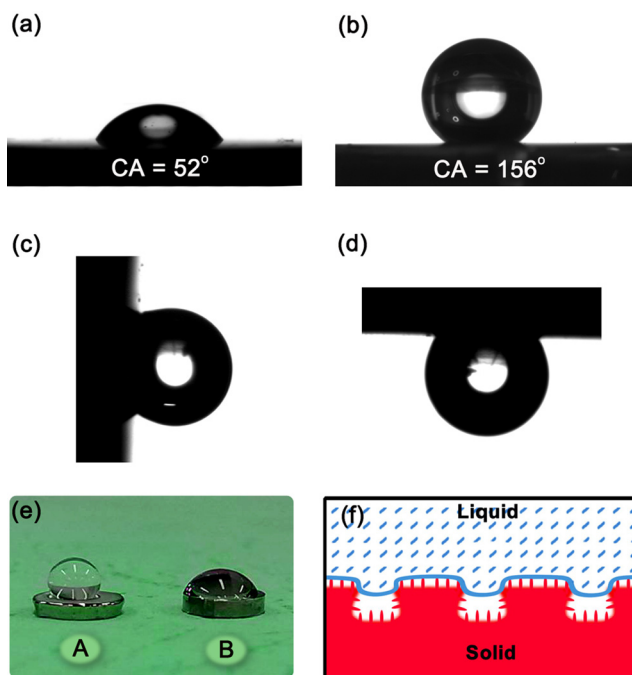


FIG. 2. (a) and (b) The CAs of the polished and micro-nano hierarchical surfaces of Pd-based MG, respectively. (c) and (d) The shapes of water droplet on the MG surface with tilted angles of  $90^\circ$  and  $180^\circ$ . (e) The photographs of water droplets on the two different surfaces, A: the micro-nano hierarchical surface and B: the polished one. (f) The wetting regime.

Recently, it has been demonstrated that superhydrophobic surfaces can be fabricated using intrinsically hydrophilic through the construction of multi-scale roughness.<sup>36–40</sup> The hierarchical structures, such as the overhang structures can prevent water from penetrating the texture arising from the capillary force. Therefore, water is in contact with a composite surface of air and solid, exhibiting apparent superhydrophobicity. In this case, the hierarchical structures consisting of nanoscale protrusions on the microscale textures with well-defined geometries can be attributed to the superhydrophobicity on the intrinsically hydrophilic MG surfaces [as illustrated in Fig. 2(f)]. Similar phenomenon can also be found in natural lotus leaves.<sup>41</sup> For the superhydrophobic lotus leaf, the intrinsic water contact angle of the wax on its surface is about  $74^\circ$ , which is contrary to the expected values of larger than  $90^\circ$ . The superhydrophobicity of these lotus leaves may be ascribed to the hierarchical structures on the surface of the lotus leaves consisting of randomly distributed micropapillae covered by branch-like nanostructures, similar to the overhang structures-induced superhydrophobicity.

The mechanical stability of the resulting superhydrophobic MG surface was first assessed qualitatively by the finger pressing. Actually, most of the natural and artificial superhydrophobic surfaces such as lotus leaf and modified low energy layer are fragile to hand touch.<sup>10</sup> The force exerted by touching would damage the fragile surface textures, making the touched area reduce or even permanently lose its superhydrophobicity. Additionally, finger contact could induce salt and oil contaminations to the surface, which is also a danger to the superhydrophobic stability. However, the MG surface remains superhydrophobic after being pressed by a finger, and the CA (about  $154^\circ$ ) has almost no change and the water drops maintain a spherical shape as

shown in Fig. 3(a). The scratch test was also conducted to study the mechanical durability of the superhydrophobic MG surface. The methodology of scratch test is illustrated in Fig. 3(b), and the MG surface was moved back and forth with a speed of 5 cm/s on the sandpaper (2000 mesh) under a constant pressure of 13 KPa. From the left in Fig. 3(c), one can see that the hierarchical structure obtained by hot-embossing still be kept after being abraded repeatedly for 100 cycles, and the water droplets still displayed special shape with a CA of  $151^\circ$ , which indicating the superhydrophobicity remains. However, when the applied force was increased to  $\sim 300$  KPa, the hierarchical structure was damaged and lose its superhydrophobicity. The right in Fig. 3(c) shows the morphology after 10 abrasion cycle under 370 kPa, and the CA of the damaged MG surface reduces to  $106^\circ$ . Therefore, the hierarchical structure on the MG surface is crucial for the superhydrophobicity. Generally speaking, the abrasion resistance which gives the mechanical stability of superhydrophobic surface is regarded as having a strong relationship with the hardness of a material.<sup>42</sup> Owing to the unique amorphous structure, MGs have much higher hardness and strength than that of the corresponding crystal alloys,<sup>20</sup> indicating a higher abrasion resistance and mechanical stability. The histogram in Figure 3(d) compares the hardness of Pd-based MG, polymers, and some commonly used crystal alloys during the fabrication of superhydrophobic surface.<sup>43</sup> We can see the MG has a higher hardness providing a better mechanical stability.

The superhydrophobic surfaces usually involve a series of chemical solutions such as the acid-base solution, and the corrosion resistance is of great importance for their practical applications. To investigate the corrosion behavior of this superhydrophobic MG at room temperature, eight different common solutions were used including: 1 mol/l hydrochloric, nitric, sulfuric, and phosphoric acid ( $\text{PH} < 1$ ), 1 mol/l potassium and sodium hydroxide ( $\text{PH} > 12$ ), Phosphate Buffered Saline (PBS) solution, and 10 wt. % highly corrosive hydrofluoric acid. For comparison, the corrosion behavior of silicon, which is a common material to fabricate superhydrophobic surfaces,<sup>44-46</sup> is also studied. According to

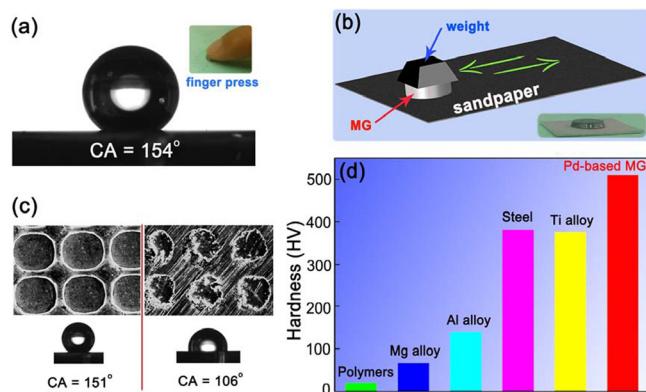


FIG. 3. Mechanical stability of the hierarchical MG surface. (a) The CA of micro-nano hierarchical Pd-based MG surface after finger press. (b) Illustration of the scratch test on sandpaper (2000 mesh). (c) The SEM images and CAs before and after the damage of the hierarchical structure by sandpaper abrasion test. (d) Hardness comparison of Pd-based MG, polymers and some crystal alloys.

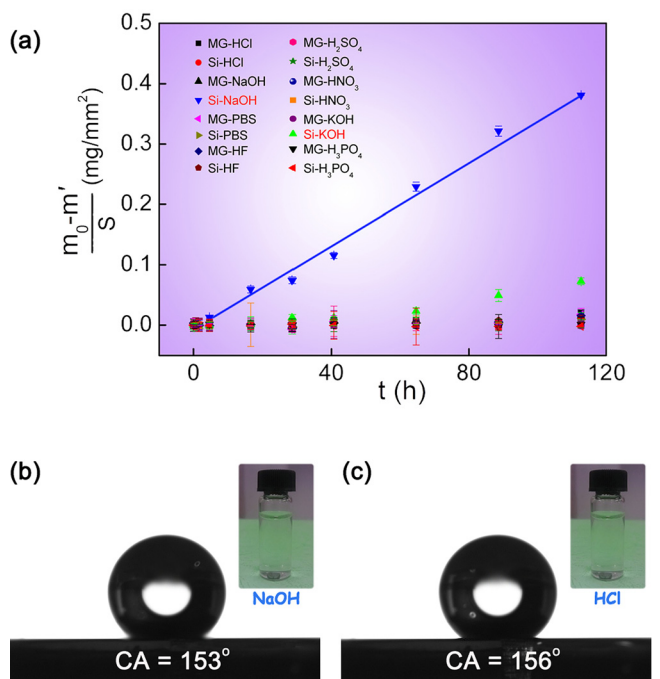


FIG. 4. (a) Mass loss of silicon and MG on per unit area in different corrosion solutions with the increase of time. (b) and (c) The CAs of micro-nano hierarchical Pd-based MG surface after soaked in the NaOH solution (1 mol/l) and the HCl solution (1 mol/l) for about 120 h.

the weight-loss method, the corrosion rate  $v$  in certain chemical solution can be expressed as  $v = \frac{m_0 - m'}{S \times t}$ , where  $m_0$  is the initial mass of a sample,  $m'$  is the mass after a corrosion time  $t$ , and  $S$  is the area that is exposed in the corrosion environment. Figure 4(a) presents the mass loss of MG and silicon on per unit area (i.e.,  $\frac{m_0 - m'}{S}$ ) with the increase of soaking time  $t$  in the aforementioned corrosion solutions. We can see both MG and silicon exhibit excellent corrosion resistance in the acid, and PBS solutions and the mass losses of MG and silicon are almost within the limits of experimental error in these solutions. However, for the strong alkaline liquids, silicon is not as stable as it is in other ones, the  $v$  reaches about  $0.00342 \text{ mg} (\text{h mm}^2)^{-1}$  in NaOH solution, which is much faster than the MG in the same condition. Figures 4(b) and 4(c) show the CAs of the hierarchical MG surfaces after being soaked in the HCl (1 mol/l) and NaOH (1 mol/l) solutions for about 120 h, respectively. We can see that the CAs and the shape of the water drops have nearly no difference compared with the untreated one, which should be ascribed to the super corrosion resistance. This indicates that MG may be an excellent promising candidate material for the fabrication of superhydrophobic surfaces used in the harsh environment. What is more, the hierarchical structure also has superior weatherability and long term environmental durability, which ensures the superhydrophobic effect would not degrade with time, temperature, humidity and so on.

In summary, Pd-based MG surfaces with micro-nano hierarchical structures are fabricated by thermoplastic forming. The resultant MG surface with well-defined hierarchical structures consisting of nanoscale protrusions on the micro-scale textures showed superhydrophobicity without low surface energy modification. These superhydrophobic MG surfaces have superior mechanical stability and corrosion

resistance. This work might be helpful for the fabrication of super stable superhydrophobic materials and extending the application fields of MGs.

The financial support of the MOST 973 of China (Nos. 2010CB731603 and 2013CB933003) and NSF of China (Grant Nos. 51271195 and 21273016), and Beijing Natural Science Foundation (No. 2122035) are appreciated. The authors are grateful for discussions with H. F. Li and S. J. Pang.

- <sup>1</sup>J. Aizenberg and P. Fratzl, *Adv. Mater.* **21**, 387 (2009).
- <sup>2</sup>B. Bhushan and Y. C. Jung, *Prog. Mater. Sci.* **56**, 1 (2011).
- <sup>3</sup>A. Solga, Z. Cerman, B. F. Strffler, M. Spaeth, and W. Barthlott, *Bioinspiration Biomimetics* **2**, S126 (2007).
- <sup>4</sup>X. Yao, Y. L. Song, and L. Jiang, *Adv. Mater.* **23**, 719 (2011).
- <sup>5</sup>P. Roach, N. J. Shirtcliffe, and M. I. Newton, *Soft Matter* **4**, 224 (2008).
- <sup>6</sup>X. Zhang, F. Shi, J. Niu, Y. G. Jiang, and Z. Q. Wang, *J. Mater. Chem.* **18**, 621 (2008).
- <sup>7</sup>Z. Guo, W. Liu, and B. Su, *J. Colloid Interface Sci.* **353**, 335 (2011).
- <sup>8</sup>K. Liu, X. Yao, and L. Jiang, *Chem. Soc. Rev.* **39**, 3240 (2010).
- <sup>9</sup>X. M. Li, D. Reinhoudt, and M. Grego-Calama, *Chem. Soc. Rev.* **36**, 1350 (2007).
- <sup>10</sup>T. Verho, C. Bower, P. Andrew, S. Franssila, O. Ikkala, and R. H. A. Ras, *Adv. Mater.* **19**, 2213 (2010).
- <sup>11</sup>C. H. Su, Y. Q. Xu, F. Gong, F. S. Wang, and C. F. Li, *Soft Matter* **6**, 6068 (2010).
- <sup>12</sup>B. Deng, R. Cai, Y. Yu, H. Q. Jiang, C. L. Wang, J. Li, L. F. Li, M. Yu, J. Y. Li, L. D. Xie, Q. Huang, and C. H. Fan, *Adv. Mater.* **22**, 5473 (2010).
- <sup>13</sup>Y. Zhu, J. Zhang, Y. Zheng, L. Feng, and L. Jiang, *Adv. Funct. Mater.* **16**, 568 (2006).
- <sup>14</sup>K. Liu, M. Zhang, J. Wang, and L. Jiang, *Appl. Phys. Lett.* **92**, 183103 (2008).
- <sup>15</sup>K. Liu, Z. Li, W. H. Wang, and L. Jiang, *Appl. Phys. Lett.* **99**, 261905 (2011).
- <sup>16</sup>I. A. Larmour, G. C. Saunders, and S. E. J. Bell, *ACS Appl. Mater. Interfaces* **2**, 2703 (2010).
- <sup>17</sup>S. T. Wang, L. Feng, and L. Jiang, *Adv. Mater.* **18**, 767 (2006).
- <sup>18</sup>A. M. Kietzig, S. G. Hatzikiriakos, and P. Englezos, *Langmuir* **25**, 4821 (2009).
- <sup>19</sup>Z. G. Guo, F. Zhou, J. C. Hao, and W. M. Liu, *J. Am. Chem. Soc.* **127**, 15670 (2005).
- <sup>20</sup>K. Liu and L. Jiang, *Nanoscale* **3**, 825 (2011).
- <sup>21</sup>Y. H. Liu, G. Wang, R. J. Wang, and W. H. Wang, *Science* **315**, 1385 (2007).
- <sup>22</sup>W. H. Wang, *Prog. Mater. Sci.* **52**, 540 (2007).
- <sup>23</sup>K. Zhao, K. S. Liu, W. H. Wang, and L. Jiang, *Scr. Mater.* **60**, 225 (2009).
- <sup>24</sup>W. H. Wang, *Adv. Mater.* **21**, 4524 (2009).
- <sup>25</sup>W. Klement, R. H. Willens, and P. Duwez, *Nature* **187**, 869 (1960).
- <sup>26</sup>B. Zhang, D. Q. Zhao, M. X. Pan, W. H. Wang, and A. L. Greer, *Phys. Rev. Lett.* **94**, 205502 (2005).
- <sup>27</sup>G. Kumar, A. Desai, and J. Schroers, *Adv. Mater.* **23**, 461 (2011).
- <sup>28</sup>J. Schroers, *Adv. Mater.* **22**, 1566 (2010).
- <sup>29</sup>K. Zhao, X. X. Xia, H. Y. Bai, and W. H. Wang, *Appl. Phys. Lett.* **98**, 141913 (2011).
- <sup>30</sup>J. Schroers, *JOM* **57**, 35 (2005).
- <sup>31</sup>J. Ma, X. Zhang, and W. H. Wang, *J. Appl. Phys.* **112**, 024506 (2012).
- <sup>32</sup>J. Ma, J. Yi, D. Q. Zhao, and W. H. Wang, *J. Appl. Phys.* **112**, 064505 (2012).
- <sup>33</sup>G. Kumar, H. X. Tang, and J. Schroers, *Nature* **457**, 868 (2009).
- <sup>34</sup>J. Yi, D. Q. Zhao, M. X. Pan, and W. H. Wang, *Adv. Eng. Mater.* **12**, 1117 (2010).
- <sup>35</sup>Y. Saotome, Y. Fukuda, I. Yamaguchi, and A. Inoue, *J. Alloys Compd.* **434–435**, 97 (2007).
- <sup>36</sup>N. Li, T. Xia, L. Heng, and L. Liu, *Appl. Phys. Lett.* **102**, 251603 (2013).
- <sup>37</sup>T. Xia, N. Li, Y. Wu, and L. Liu, *Appl. Phys. Lett.* **101**, 081601 (2012).
- <sup>38</sup>J. Yi, L. S. Huo, D. Q. Zhao, H. Y. Bai, and W. H. Wang, *Sci. Chin. G* **55**, 609 (2012).
- <sup>39</sup>A. Marmur, *Langmuir* **24**, 7573 (2008).
- <sup>40</sup>L. Cao, H. H. Hu, and D. Gao, *Langmuir* **23**, 4310 (2007).
- <sup>41</sup>L. Cao, T. P. Price, M. Weiss, and D. Gao, *Langmuir* **24**, 1640 (2008).
- <sup>42</sup>Y. T. Cheng and D. E. Rodak, *Appl. Phys. Lett.* **86**, 144101 (2005).
- <sup>43</sup>H. A. Gardner and G. G. Sward, *Paint Testing Manual*, 13th ed. (ASTM International, California, 1972), p. 301.
- <sup>44</sup>W. H. Wang, *J. Appl. Phys.* **110**, 053521 (2011).
- <sup>45</sup>T. Baldacchini, J. E. Carey, M. Zhou, and E. Mazur, *Langmuir* **22**, 11 (2006).
- <sup>46</sup>M. F. Wang, N. Raghunathan, and B. Ziaie, *Langmuir* **23**, 5 (2007).